Technical report

Application of thermal plasma torch for steel heat-treatment furnaces: Results from the pilot-scale test

Ilman Nuran Zaini – *KTH Royal Institute of Technology*

Rikard Svanberg – *KTH Royal Institute of Technology*

Weihong Yang – *KTH Royal Institute of Technology*

Daniel Sundberg – *ScanArc AB*

Kristofer Bölke – *Linde Gas AB*

TABLE OF CONTENT

LIST OF FIGURES

LIST OF TABLES

1   INTRODUCTION

1.1 Background

The electrification of furnaces in the steel industry faces a big challenge as a significant portion of high-temperature heat is required to meet the operational need. These requirements are challenging to comply with conventional electrified heating (e.g., resistance and induction heating). Hence, the use of plasma torches as the route for electrification is gaining interest. The main advantages of plasma torches compared to other alternatives are the high temperature in the plasma jet, the plasma's high energy density, and the possibility of using different plasma gases depending on the desired application. Replacing fossil fuel burners with plasma torches can also lead to lower operating costs and greenhouse gas emissions. Other advantages include controlled process chemistry, small installation sizes and rapid start-up and shutdown features [1]. However, the main difference when introducing plasma torches is that there will be no combustion reaction in the firing zones, which changes the process gas composition and may include higher NO_x emission[2]. Hence, the selection of certain plasma carrier gas and other operating parameters is crucial to achieving plasma-heated furnaces with high efficiency and a low emission level.

In this study, pilot-scale trials were performed to investigate the possibility of plasma torch application for steel-heat treatment furnaces. The performance of the plasma system was evaluated under different operating parameters.

1.2 Objectives

This pilot-scale study aims to evaluate the performance of the plasma heating system under different carrier gases. The evaluation is carried out for the following aspects.

- NO_X emission in the flue gas.
- Ability to reach a sufficient furnace temperature.
- Ability to properly heat the steel samples.

---

[1] Lindén E, Thureborn E. Electrification of the heat treatment process for iron ore pelletisation at LKAB. Chalmers University of Technology, 2019.
[2] Lindén E, Thureborn E. Electrification of the heat treatment process for iron ore pelletisation at LKAB. Chalmers University of Technology, 2019.

2   FURNACE CONFIGURATIONS AND TRIAL PROCEDURES

2.1 Pilot-scale heating furnace

The trials were conducted at a testing ScanArc's facility in Hofors. A furnace with the furnace body's outer dimension of 3.5 x 2.2 x 2.2 m was used (see Fig. 1). The furnace body was isolated with a 0.3 m thick layer of ceramic fibre material. There were also three small doors in the furnace body to load and unload the steel samples to/from the chamber.

A 250 kW DC plasma torch was installed to a side of the furnace as seen in Fig. 2. In addition, a tuyere was added as an inlet for the forma gas. Forma gas is added as a secondary carrier gas other than the plasma gas itself. In contrast with plasma gas, forma gas does not flow through the core of the plasma torch. Instead, it will mix with the plasma gas at the torch outlet to form the plasma jet.
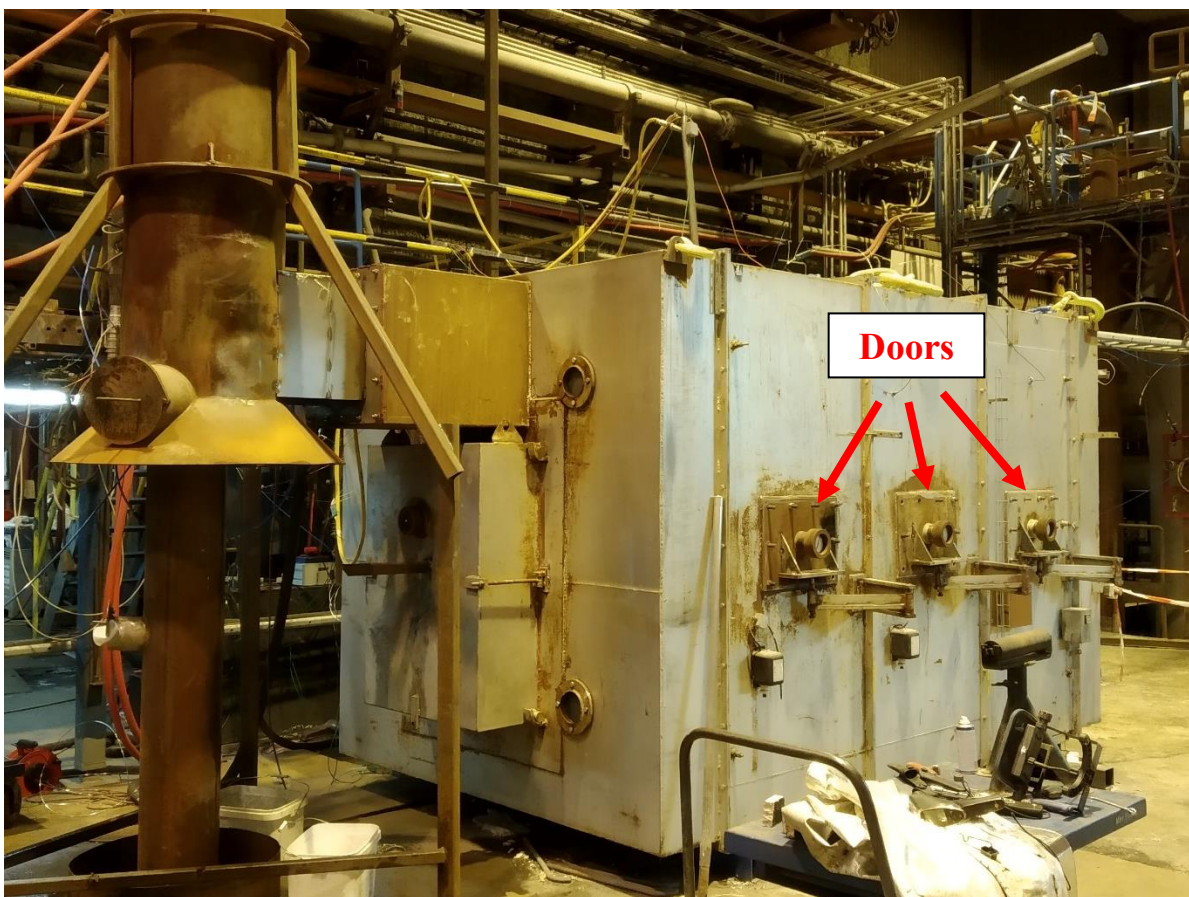
Fig. 1. The pilot-scale furnace installed for the trial.
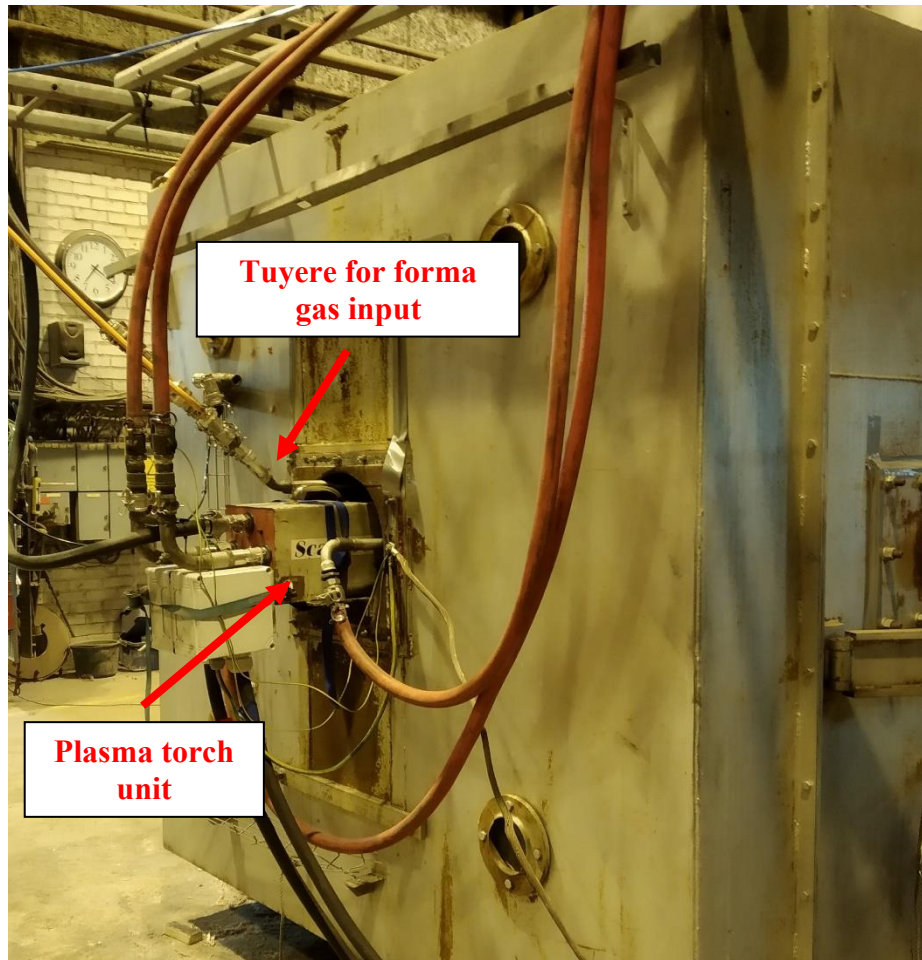
Fig. 2. The installed plasma torch unit used for the trial.

2.2 Operating parameters

The pilot-scale study consisted of 5 days of trials that were conducted in November 2020. Table 1 shows the details of those trials. For each trial, a different plasma and forma gas mixture were used to investigate the effect of these gases on the steel heat-treatment performance, as well as the produced emission. For each case, the trial began with a preheating stage at which the plasma torch was turned on to heat the furnace from a room temperature to the maximum target temperature of 1200 ºC. After that, the furnace was maintained at approximately the same temperature by adjusting the plasma torch power or carrier gas flow. The data of plasma torch power, heat loss due to cooling of the plasma torch, furnace temperature, steel sample temperature, and gas emission were monitored and recorded throughout the test.

After the target temperature was obtained, the steel samples (provided by SSAB, OVAKO, and Outokumpu) were placed into the furnace at three different positions, as shown in Fig. 4. These sample positions are located in parallel with the furnace's doors, and each of them represents a specific residence time of the steel heat treatment, which are 60, 75, 120, or 300 min. In addition to those aforementioned samples, a muffle sample provided by Höganäs was placed at sample position 1 as shown in Fig. 4. The sample was always kept inside the furnace during the whole trials. Thermocouples were attached on the surface of the sample to monitor its temperature profile.

Table 1. Details of the pilot-scale trials.

| Case number | Date of trial | Carrier gas input | |
		Plasma gas	Forma gas
1	November 10, 2020	Air	Air, LPG
2	November 11, 2020	CO_2	CO_2
3	November 17, 2020	N_2	N_2
4	November 18, 2020	CO_2	CO_2, H_2O
5	November 19, 2020	N_2	N_2, H_2O

Fig. 3. Loading the steel samples through furnace's windows.

2.3 Temperature measurements

The furnace chamber temperature was measured at six different locations, namely TT_1W, TT_2W, TT_3W, TTN, TT_4E, and TT_3E as shown in Fig. 4. The temperature data from these thermocouples were then used to characterise the temperature distribution of the chamber. Specifically, the temperature distribution is quantified by using T_{avg} and ΔT. The value of T_{avg} represents the average temperature obtained from those six thermocouples at a certain time t. Meanwhile, ΔT is defined as follows,

$$\Delta T = T_{max}(t) - T_{min}(t) \qquad \text{(Eq. 1)}$$

where $T_{max}(t)$ and $T_{min}(t)$ are the maximum and minimum temperature values between TT$_1$W, TT$_2$W, TT$_3$W, TTN, TT$_4$E, and TT$_3$E thermocouples at a certain time t, respectively.
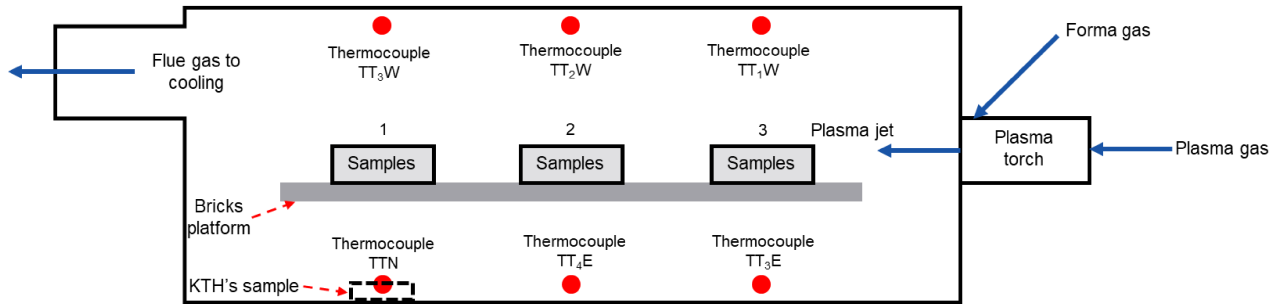
Fig. 4. Schematic diagram of the location of the steel samples and thermocouples inside the furnace.

Moreover, an additional steel sample provided by KTH was placed in the chamber as indicated in Fig. 4. It was always kept inside the furnace throughout the whole trials (i.e., from the beginning of Case 1 until the end of Case 5). This sample had a cylindrical shape with a diameter of 170 mm and a height of 110 mm, as shown in Fig. 5. A thermocouple was planted at the core of the sample, and the temperature data were recorded throughout the test. In addition, two thermocouples were also attached on the Outokumpu's samples located in sample position 3 in Fig. 4 to collect their temperature data during the trials.

Fig. 5. The steel sample provided by KTH.

2.4 Total heat flux measurements

A total heat flux (THF) measurement probe provided by KTH was used to measure the total radiation and convection heat flux in the furnace. The probe's tip consisted of two type-K thermocouples (see Fig. 6), which was placed at the centre of the furnace chamber. The value of THF was then calculated based on the temperature difference recorded by those thermocouples.
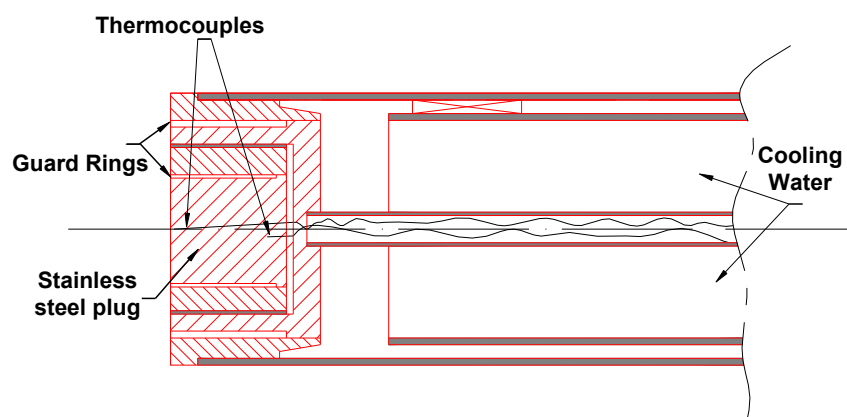
Fig. 6. Schematic diagram of the total heat flux meter probe used during the trial.

2.5 Flue gas analysis

The flue gas emitted from the furnace chamber was analysed using the gas analysers provided by both Linde and KTH. These gas analysis instruments can detect NO, NO_2, O_2, CO, and CO_2 as dry gases with the measurement ranges, as shown in Table 2 and Table 3. During the test, both gas analysers show a similar result, as long as they are within the measurement range. Nevertheless, considering the better measurement range, only the gas data obtained from Linde's instrument is presented in this report. The total flue gas flow rate (in Nm^3/h) was calculated by considering the additional air due to the leaks. This was done by adding a certain amount of N_2 based on the concentration of excess O_2 in the data.

Table 2. Specifications of the Linde's gas analyser.

Gases	Detector	Measurement range
O_2	ABB Magnos 206	0–100%
CO	ABB Uras 26	0–10000 ppm
CO_2	ABB Uras 26	0–100%
NO	ABB Limas 11	0–5000 ppm
NO_X	ABB Limas + NO_X-converter	Maximum NO_2 300–400 ppm for >95% conversion.

Table 3. Specifications of the KTH's gas analyser.

Gases	Detector	Measurement range
O_2	Sick GMS 810	0–25%
CO	Sick GMS 810	0–50000 ppm
CO_2	Sick GMS 810	0–25%
NO	Sick GMS 810	0–2000 ppm

In this report, the total NO_X emission is defined by expressing the NO and NO_2 as NO_2 equivalents. Hence, the calculation formula for the total NO_X emission can be written as follows,

$$Total\ NO_X = (m_{NO}\ x\ 1.53) + m_{NO2} \qquad \text{(Eq. 2)}$$

where m_{NO} is the amount of NO (mg) in the flue gas and m_{NO2} is the amount of NO_2 (mg) in the flue gas. Meanwhile, the constant value of 1.53 is obtained based on the molecular weight ratio of NO_2 to NO.

3 RESULTS

3.1 Plasma torch efficiency and measured THF

Table 4 shows the average values of the operating parameters calculated after the steel samples were placed into the furnace chamber until the final residence time of 300 min. It should be noted that during the initial stage of the test of some cases, the furnace was heated with additional LPG or different plasma power to make sure it could reach the desired operating temperature. Hence, the operating parameter values in that stage might differ from those presented in Table 4.

As shown in Table 4, different plasma gas carriers affect plasma power efficiency. In general, the plasma efficiency trend is related to the plasma gas carrier's specific heat capacity, in which a higher specific heat capacity causes a higher efficiency. The results from the trials also confirm this trend when there is no LPG added in the process. To be specific, both plasma efficiency and specific heat capacity of the plasma gas carrier at a high temperature (>3000 K, see Table 5) follow the same order of $CO_2 > N_2 >$ air. Hence, without the presence of additional energy from LPG, the use of CO_2 as a plasma gas carrier resulted in the highest plasma torch efficiency than other gas carrier tested in this study. However, it should be noted that the plasma torch used in this study was not specifically adjusted to the tested gases. In the real application, the plasma torch can be modified for a specific carrier gas composition to obtain a higher efficiency.

Table 4. Average values of the operating parameters and measured heat flux during 300 min of steel heat-treatment.

Case	Plasma power (kW)	Heat loss (kW)	Energy to the furnace (kW)	Plasma efficiency (%)	Total carrier gas input (Nm³/h)					Measured THF in the furnace (W/m²)
					Air	LPG	CO₂	N₂	H₂O (kg/h)	
1	119.1	50.0[b]	69.1 (89.2[a])	58.0 (75.0[a])	76.7	2.9				195.9
2	184.6	43.1	141.5	76.7			64.0			182.0
3	214.2	85.2	129.0	60.2				65.4		134.6
4	191.0	43.4	147.6	77.3			60.4		36	127.9
5	241.7	93.0	148.7	61.5				107.8	36	161.2

[a]include LPG (25 MJ/Nm³)
[b]heat loss of LPG is not included

Table 5. Specific heat capacity of different carrier gases[3].

Gas medium	Specific heat capacity C_P (kJ/kg K) at different temperatures (1 bar)					
	300 K	1000 K	2000 K	3000 K	4000 K	5000 K
Air	1.006	1.142	1.250	1.290		
CO_2	0.846	1.234	1.371	1.414	1.437	1.455
N_2	1.040	1.167	1.284	1.323	1.342	1.355
H_2O		2.293				

The measured THF value represents the total heat flux due to both radiation and convection. Fig. 7 shows the plot of several THF values against the furnace temperature (T_{avg}) that were collected when the furnace was heated from the room temperature to the maximum target temperature of 1200 °C. As shown in the figure, the THF value correlates well with the furnace temperature, as its value generally increase with the increase of furnace temperature. These results confirm the significance of the radiation heat flux over the convection one.

Furthermore, to know the effect of convection heat flux a comparison between THF values at approximately the same temperature is performed. Fig. 8 presents the THF values obtained when the furnace is maintained at the target temperature between 1150–1200 °C. The data presented in the figure are taken randomly from the sample to illustrate the variation of the THF value. As can be seen in the figure, the values of THF varies significantly even though the surrounding temperature are approximately similar. For instance, as indicated in the figure, point "A" has a 11% higher THF value than "B" despite the only 6 °C different in the T_{avg}. This is possible due to "A" has a higher CO_2 flow (98.8 Nm³/hr) and plasma power (267.5 kW) than that of "B" (CO_2 flow of 78.3 Nm³/hr and plasma power of 162.6 kW). A same trend can also be observed between Case 3 and Case 5 where they have a different flow rate of N_2. As indicated by point "C" of Case 5, operating the plasma torch with a N_2 flow of 101.0 Nm³/hr and a plasma power of 230.0 kW results in a THF value of 172.4 W/m². This value is 23% than the THF value of point "D" in which the plasma torch is operated at a N_2 flow of 62.0 Nm³/hr and a plasma power of 209.0 kW. Furthermore, the average THF value of Case 2 is notably higher than Case 4 despite Case 4 having a similar flow of CO_2 with addition of H_2O. This result might be due to the higher gas amount circulated inside the furnace as there were more air leaks during Case 2 test. Specifically, the amount of dry flue gas in Case 2 is around 79 Nm³/h, whereas Case 4 only produces 59 Nm³/h of flue gas. The variation of THF values might also be affected by the plasma jet behavior under different carrier gas composition; however, more studies should be done to confirm this explanation.

In general, Case 1 has the highest average value of THF (193.9 W/m²) at T_{avg} values between 1150–1200 °C. This is followed by Case 2, 5, 4, and 3 that have an average THF value of 180.1, 172.4, 157.6, and 137.2 W/m², respectively. This trend is similar with the total average value of THF obtained during the full 300 min of steel heat-treatment as presented in Table 4.

---

[3] https://www.engineeringtoolbox.com/ n.d.
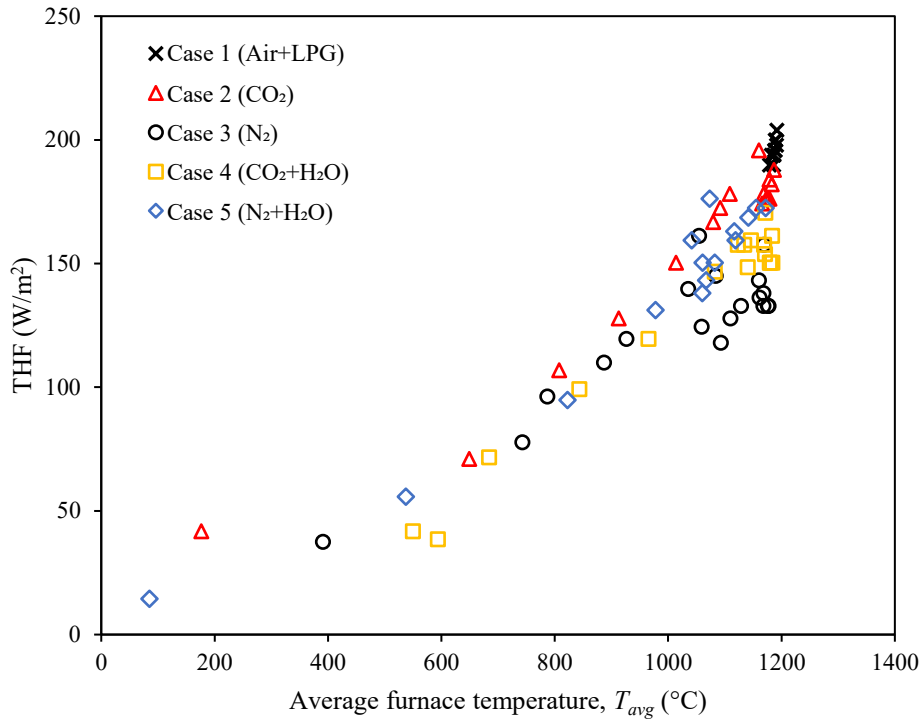
Fig. 7. The relation between the measured THF value and furnace temperature.
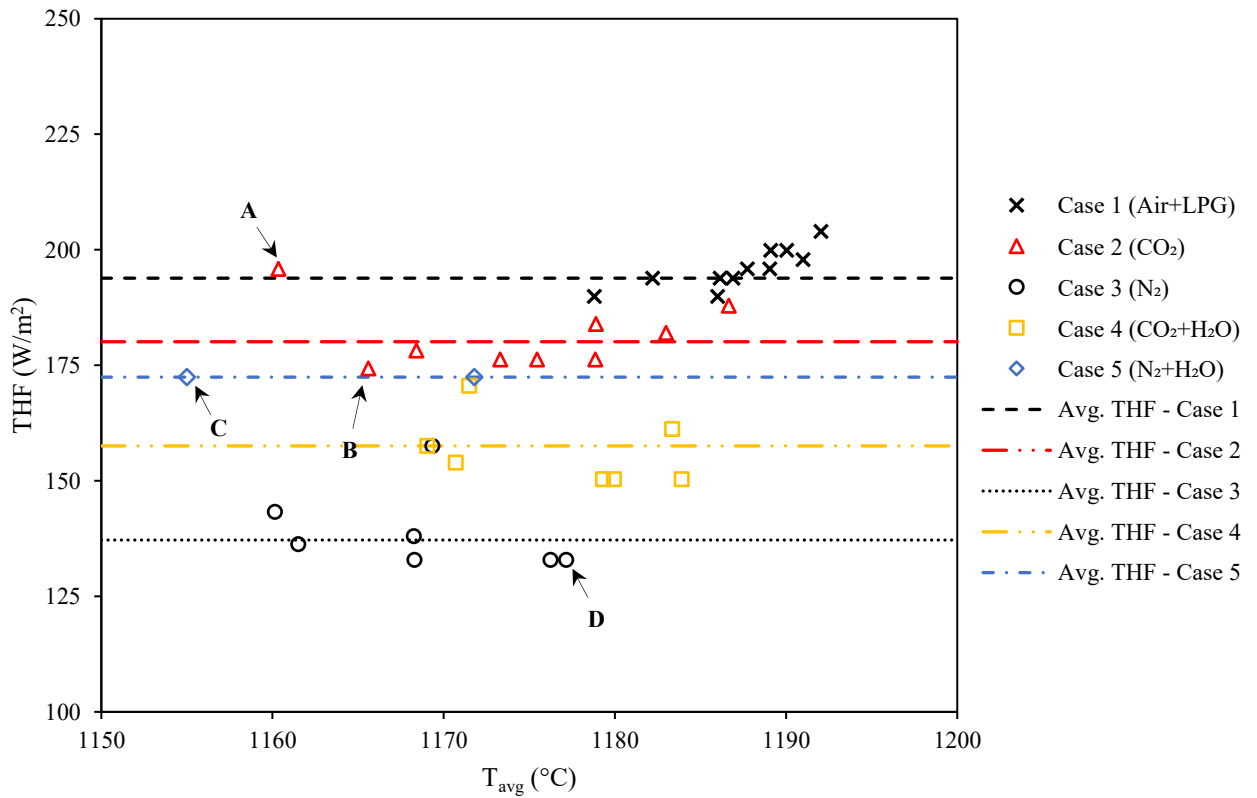
Fig. 8. The THF values obtained when the furnace is maintained at the target temperature between 1150–1200 °C.

3.2 The temperature profile of the furnace

3.2.1 Air and LPG as carrier gas

Fig. 9. Temperature profiles of the pilot furnace with air and LPG as plasma gases during steel heating.

Table 6. The temperature distribution inside the pilot furnace with air and LPG as plasma gases.

Time	Plasma torch parameters		Average values of furnace parameters (°C)			
	Power input (kW)	Carrier gas (Nm³/h)ᵃ	T_{avg}	ΔT_{max}	ΔT_{min}	ΔT_{avg}
8:40-9:10	200.1	79.5	1173	41	22	34
Sample in						
9:30-10:15	134.6	81.9	1180	29	21	25
Sample out after 60 & 75 min						
10:30-11:10	124.5	81.5	1185	22	16	20
Sample out after 120 min						
11:20-14:05	113.6	78.5	1188	47	16	25
Sample out after 300 min						

ᵃLPG is included at 2.9 Nm³/h

The temperature profile of the furnace interior during Case 1 test on the first day of the trial is shown in Fig. 9. In this case, air and LPG were used as the plasma and forma gases, respectively. As seen in the figure, the use of both air and LPG in the plasma generator provided a relatively good heating process as the furnace could reach the desired operating temperature in a reasonable time. Specifically, the furnace could reach ±1200 ºC in approximately 90 min. Also, temperature fluctuations can be seen in the graph where the temperature steeply decreased

15

and then increased in a short time. These fluctuations represent the loading and unloading of the steel samples during the trial.

Table 6 shows a summary of the temperature distribution of the furnace interior. The data summary is presented for different steps of the steel/sample heating process. In general, the T_{avg} values remain constant in the range of 1180–1188 ºC, which indicates a stable operating condition during the trials. On the other hand, the ΔT_{avg} values range between 20 – 25 ºC for each heating steps.

3.2.2 CO_2 as carrier gas

Fig. 10. Temperature profiles of the pilot furnace with CO_2 as plasma gases during steel heating.

Table 7. The temperature distribution inside the pilot furnace with CO_2 as plasma gases.

Time	Plasma torch parameters		Average values of furnace parameters (°C)			
	Power input (kW)	Carrier gas (Nm³/h)*	T_{avg}	ΔT_{max}	ΔT_{min}	ΔT_{avg}
10:54-11:13	267.2	76.7	1051	45	50	54
Sample in						
11:37-12:15	234.8	69.8	1171	45	29	37
Sample out after 60 & 75 min						
12:45-13:18	190.4	61.1	1181	31	24	28
Sample out after 120 min						
13:37-16:14	168.7	60.5	1172	27	20	22
Sample out after 300 min						

Fig. 10 shows the furnace temperature data from Case 2 in which CO_2 was used as both plasma and forma gases. As shown in the figure, the furnace could be heated up to the desired operating temperature of ±1200 ºC in about ~100 min. This time duration is only slightly longer

16

than that of LPG-assisted air plasma generator as presented above. The T_{avg} values range between 1171–1181 °C during the operation, as shown in Table 7. Furthermore, the trial exhibited a slightly higher range of ΔT_{avg} values than the previous day trial as they range between 22–37 °C.

3.2.3 N_2 as carrier gas

Fig. 11 presents the furnace interior's temperature profile during the heating by using N_2 as the plasma and forma gases. This trial shows that the heating rate of the furnace was significantly lower than that of air- or CO_2-based plasma generator from the previous days of the trial. As seen in the figure, it took approximately 90 min to heat the reactor from the initial temperature to 900 °C. This value was significantly longer than the case of air+LPG- and CO_2-based plasma generator, which only needs about 10 and 25 min, respectively, to reach the same temperature. Therefore, in the middle of the preheating process, the N_2 flow was switched to 5.0 Nm^3/h of LPG and 30.0 Nm^3/h of air to enhance the heating rate of the furnace. This was done between 9.30–10.00 AM as can be seen in the figure. As a result, the furnace temperature increased significantly and could easily reach the desired operating temperature. The LPG flow was then shut down, and the plasma torch was operated back to 100% of N_2 before the initial sample loading.

Table 8 presents the temperature distribution of the furnace. Despite the slow heating process at the beginning of the trial, the T_{avg} values remain relatively constant between 1166–1171 °C after the furnace reached the steady condition. Nevertheless, the ΔT_{avg} values are higher than the case of air- or CO_2 atmosphere, which are between 32–45 °C. These values could be reduced to 27–29 °C by increasing the flow of the N_2 as shown in the table during the period from 15.07 to 15.23. These results may indicate that the degree of the furnace's temperature uniformity is lower when N_2 is used in the plasma torch than that of air or CO_2.
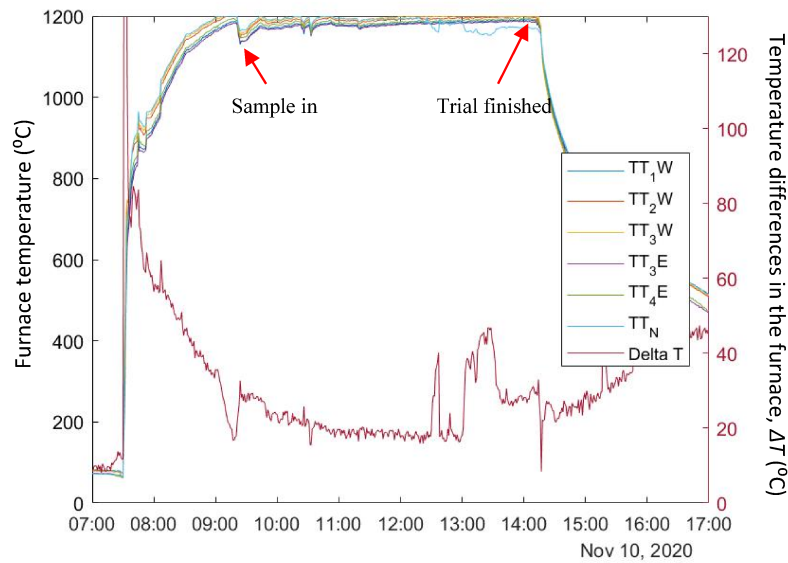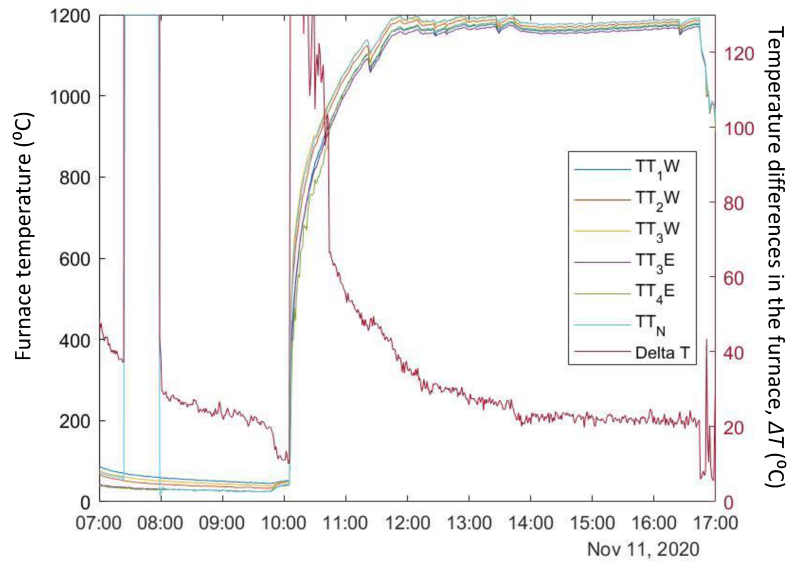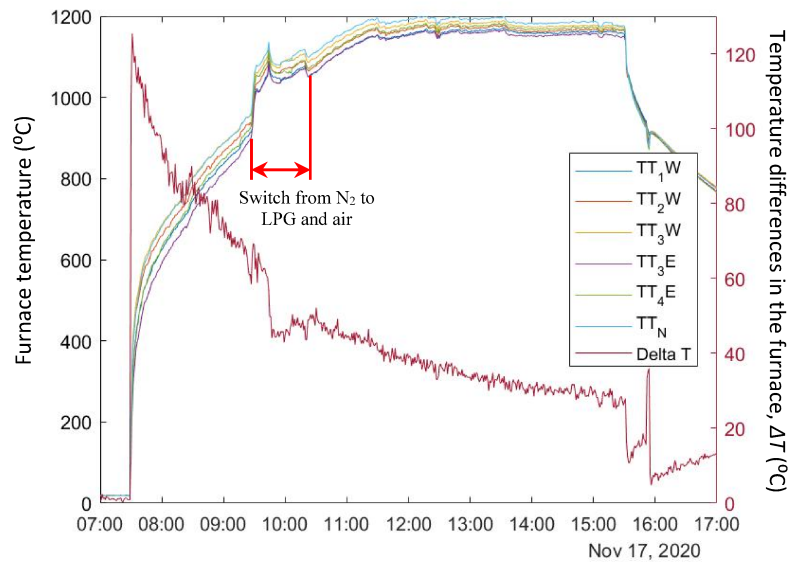

Fig. 11. Temperature profiles of the pilot furnace with N_2 as plasma gases during steel heating.

Table 8. The temperature distribution inside the pilot furnace with N_2 as plasma gases.

Time	Plasma torch parameters		Average values of furnace parameters (°C)			
	Power input (kW)	Carrier gas (Nm³/h)	T_{avg}	ΔT_{max}	ΔT_{min}	ΔT_{avg}
8.55-9.18	244.2	106.3	878	77	66	71
9.29-9.37	245.1	114.7ª	1048	67	59	63
9.49-10.06	256.1	97.3ª	1066	50	43	46
Sample in						
10.34-11.15	257.6	80.3	1131	49	42	45
Sample out after 60 & 75 min						
11.42-12.08	227.5	70.5	1169	41	37	39
Sample out after 120 min						
12.36-14.57	189.4	57.7	1171	38	28	32
Plasma gas flow is increased						
15.07-15.11	181.5	67.0	1169	30	29	29
Forma and plasma gas flow are increased						
15.16-15.23	178.3	86.3	1166	30	25	27
Sample out after 300 min						

ªLPG is added at 5.0 Nm³/h.

3.2.4 CO$_2$ and H$_2$O as carrier gases

Fig. 12 presents the furnace's temperature profile during the trial with CO_2 as the plasma gas and H_2O addition as a forma gas. At the beginning of the trial, the plasma generator was operated with 100% CO_2 without any H_2O. After the furnace reached a certain temperature, the H_2O flow was then started to be added through the tuyere. After the trial reached the steady operating condition, the maximum recorded T_{avg} value can reach 1181 ºC, as shown in Table 9. Meanwhile, the ΔT_{avg} value ranges between 23–37 ºC, which is similar to that of trial with an only CO_2 atmosphere. This may suggest that the amount of H_2O added to the process did not significantly change the furnace's temperature distribution.
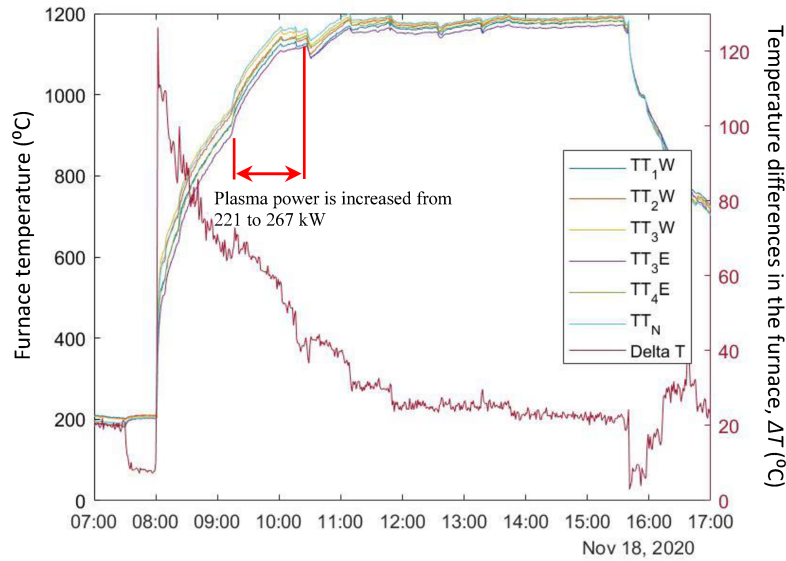
Fig. 12. Temperature profiles of the pilot furnace with CO_2 as plasma gas and H_2O as forma gas during steel heating.

Table 9. The temperature distribution inside the pilot furnace with CO_2 as plasma gas and H_2O as forma gas.

Time	Plasma torch parameters		Average values of furnace parameters (°C)			
	Power input (kW)	Carrier gas (Nm³/h)ᵃ	T_{avg}	ΔT_{max}	ΔT_{min}	ΔT_{avg}
Sample in						
10.40-11.20	233.4	70.8	1164	43	29	37
Sample out after 60 & 75 min						
11.50-12.25	186.9	65.2	1167	27	24	25
Sample out after 120 min						
12.50-13.08	187.9	65.6	1173	27	24	25
Sample out after 170 min						
13.37-15.23	174.4	61.7	1181	27	20	23
Sample out after 300 min						

ᵃsum of CO_2 only, exclude H_2O flow of 36 kg/h

3.2.5 N_2 and H_2O as carrier gases

The last day of the pilot trial was dedicated to testing N_2 and H_2O mixtures for generating the plasma jet. Based on the experience from the previous case of the N_2 plasma torch, LPG was added to the plasma torch to assist the heating process before the sample loading into the furnace. The plasma generator was then operated with only N_2 and H_2O after the furnace reached the temperature target. As shown in Fig. 13, the furnace temperature dropped significantly soon after the gases were changed from LPG to N_2-H_2O mixture. Thereafter, the temperature gradually increased toward the end of the trial. Table 5 shows the values of T_{avg}

were recorded between 1070 to 1147 °C during the trial, which is among the lowest value range compared to other trials done in this project. Moreover, the ΔT_{avg} of the furnace also higher than other cases as it reached 49–66 °C; suggesting that the furnace had a less uniform temperature distribution during the test. These results may indicate that the combination of N_2 and H_2O used in this trial is least favourable than other gas combinations in terms of the furnace's heat transfer.
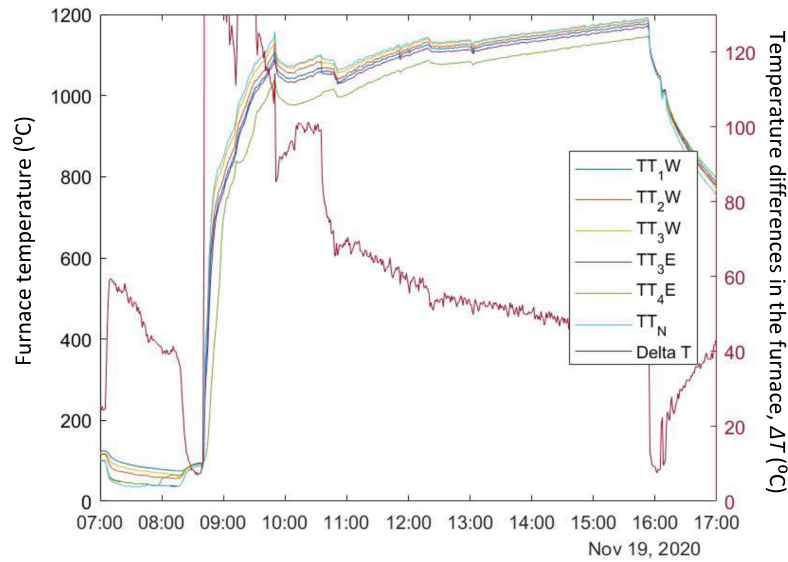
Fig. 13. Temperature profiles of the pilot furnace with N_2 as plasma gas and H_2O as forma gas during steel heating.

Table 10. The temperature distribution inside the pilot furnace with N_2 as plasma gases and H_2O as forma gas.

Time	Plasma torch parameters		Average values of furnace parameters (°C)			
	Power input (kW)	Carrier gas (Nm³/h)	T_{avg}	ΔT_{max}	ΔT_{min}	ΔT_{avg}
10.00-10.30	257.7	107.8[a]	1051	101	93	98
10.30-10.42	258.0	105.3[a]	1062	101	74	85
Sample in						
10.52-11.44	259.6	115.2[b]	1070	70	60	66
Sample out after 60 & 75 min						
12.01-12.21	256.3	112.5[b]	1117	60	52	57
12.21-12.52	233.0	105.4[b]	1115	56	51	54
Sample out after 135 min						
13.10-15.40	235.0	105.0[b]	1147	53	44	49
Sample out after 300 min; H₂O flow is doubled						
15.53-15.59	235.0	104.5[b]	1083	13	8	10

[a]sum of N_2, air, and LPG
[b]sum of N_2 only, exclude H_2O flow

3.2.6 Summary of the furnace temperature results

Temperatures at a different side of the furnace interior have been collected to investigate the effect of these different gas mediums on the furnace's temperature distribution. In general, the results indicated that different gas combination used as either plasma or forma gas significantly affect the heating process. This trend consequently results in different temperature distributions of the furnace interior. Fig. 14 and Fig. 15 respectively summarise the furnace temperature, T_{avg}, and the average temperature difference, ΔT_{avg}, obtained during different tests.

Based on the results of the conducted tests, the following conclusions can be made.

- Different gas combinations used in generating the plasma jet significantly affect the heating performance of the furnace interior.
- The use of CO_2 or a mixture of air–LPG in the plasma generator provides a sufficient heating performance, in which the latter can provide the highest heating rate and the most uniform temperature distribution.
- CO_2 has a great potency to be used as a plasma carrier gas as it can heat the furnace properly without the need of additional external fuel (e.g. LPG).
- Combination of N_2 and H_2O is least favourable due to the poorer temperature distribution and lower heating rate.
- At the end of the trials, the temperature of the furnace varied approximately 20 °C, which is within an acceptable range.
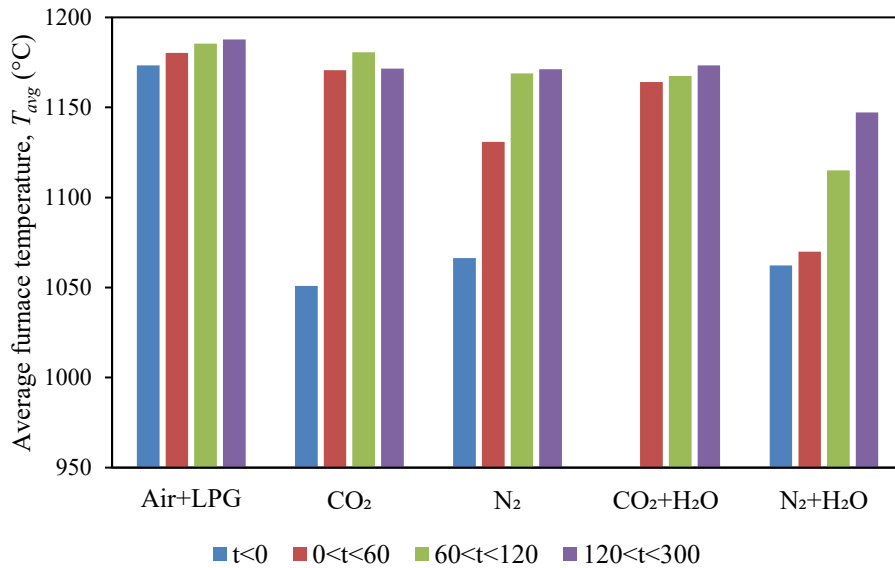
Fig. 14. Average furnace temperature (T_{avg}) at different atmospheres and times (t, in min).
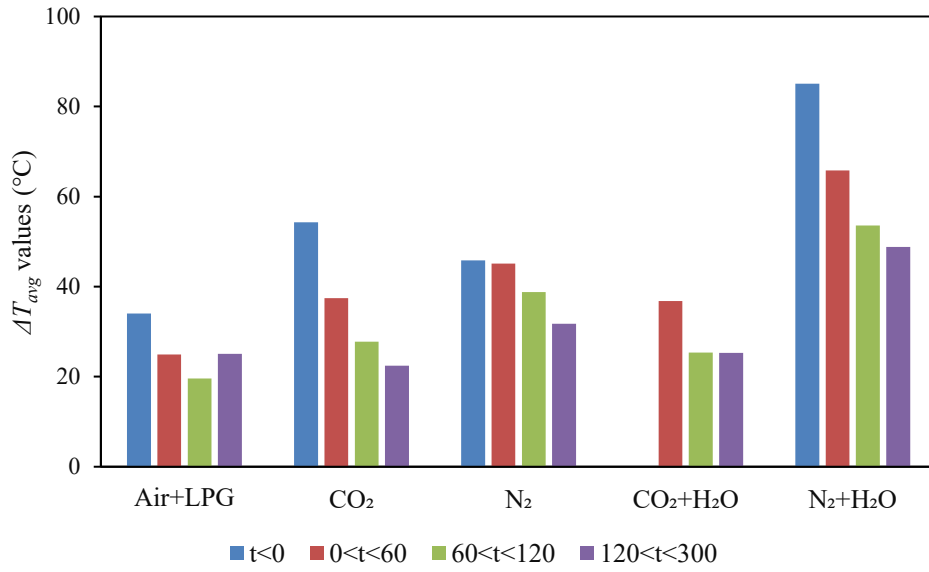
Fig. 15. Average temperature differences in the furnace (ΔT_{avg}) measured at different atmospheres and times (t, in min).

3.3 The temperature of the steel sample

Fig. 16 shows the KTH's steel sample core temperature during the preheating stage of Case 3, 4, and 5. In general, the core temperature could reach ~1200 °C in all cases, as shown in the figure. It suggests that the steel sample could be uniformly heated to the same temperature of the furnace chamber. Nevertheless, the time needed to reach the target temperature was significantly different among those cases, which was similar to the furnace temperature trend, as explained previously. For instance, in Case 3, the time needed to heat the steel core from 200 to 850 °C under a N_2 atmosphere was around 93 min. Meanwhile, in Case 4, it took approximately 67 min to heat the steel core under a CO_2-H_2O atmosphere for the same temperature range. Furthermore, as explained previously, air and LPG were added during the preheating stage of Case 5 to improve the rate of N_2-H_2O based plasma heating. Consequently, the steel sample's core temperature could be elevated faster than in other cases as it took only 32 min to reach 850 °C from 200 °C. However, the temperature started to decrease after the carrier gas was changed to N_2-H_2O before it started to increase in the second half of the test gradually. Therefore, it can be concluded that there is a similarity between the trend of the steel sample and the furnace heating rate. Specifically, the combination of air and LPG tends to generate the highest heating rate, followed by CO_2 and N_2, respectively.

Fig. 17 shows the surface temperature of the Outokumpu's sample during Case 4 and 5 trials. As shown in the figure, when the furnace temperature reached its steady state, the surface temperature is approximately 30 °C higher than the average value of the furnace temperature T_{avg}. As the sample was positioned closer to the plasma jet, the results may suggest the higher atmosphere temperature at a position closer to the centreline of the chamber.
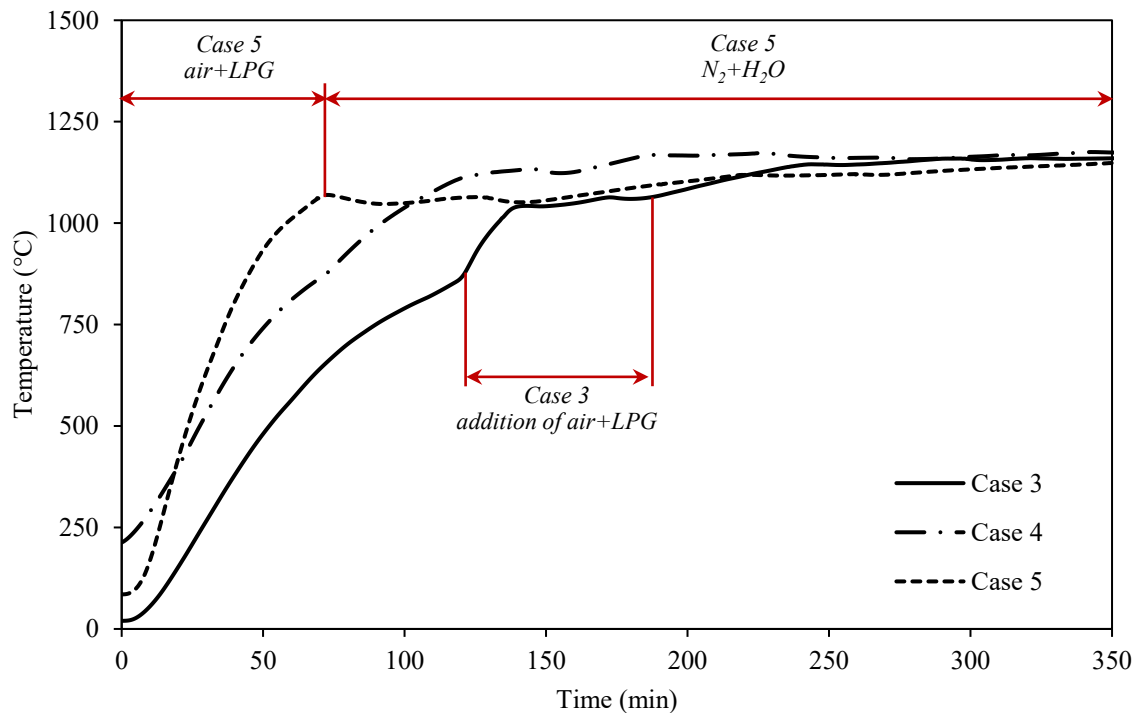
Fig. 16. The temperature of the core of the KTH's steel sample obtained during the preheating stage of Case 3, 4, and 5.
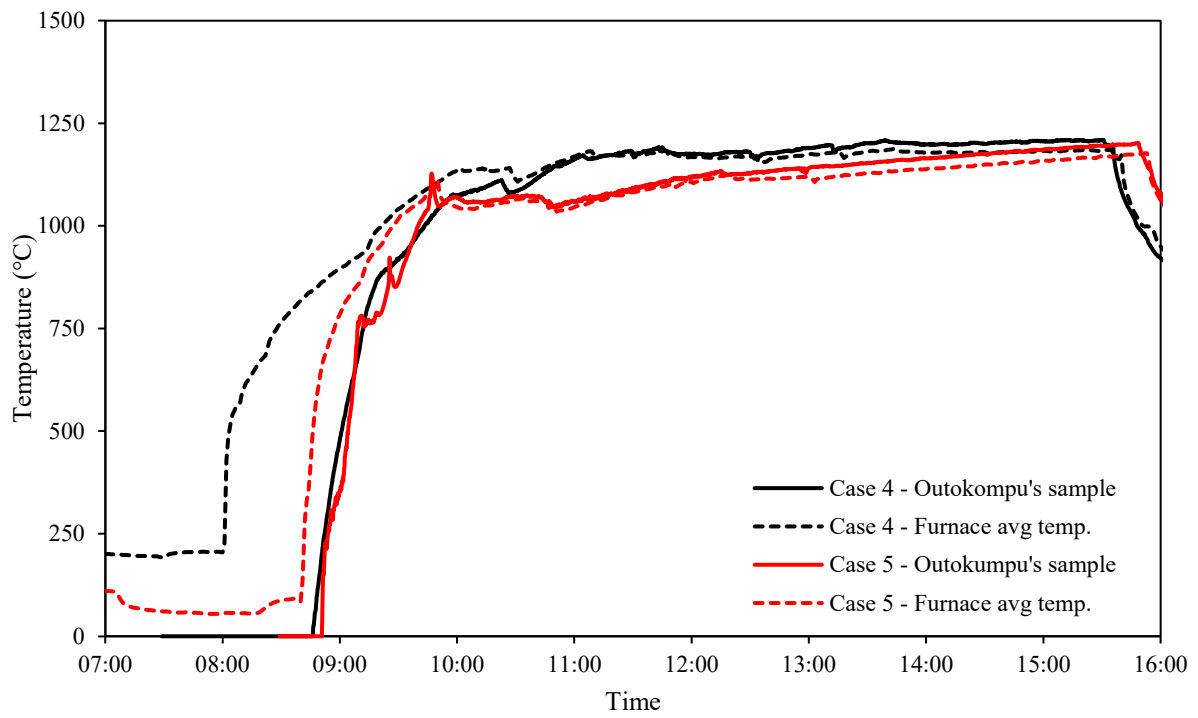
Fig. 17. The surface temperature of the Outokumpu's sample compared to the furnace average temperature (T_{avg}).

3.4 Emissions

3.4.1 Air and LPG as carrier gases

Table 11 shows the average values of flue gas composition as detected by the gas analyser during the steel heat treatment trial of Case 1. In Case 1, the plasma and forma gas input consist of air and LPG. As a result, the flue gas contains a significant amount of CO_2 emission due to LPG combustion. The CO_2 concentration is approximately 7.7 vol%. Moreover, the presence of air at a very high-temperature plasma generation causes thermal NO_X formation. Consequently, the amount of NO_X emission of Case 1 is significantly higher compared to other cases. As shown in Table 12, the total NO_X emission ranges between 18 724–21 091 mg/Nm^3 based on the equivalent value of the CH_4 combustion with 3% excess O_2. The details of the NO_X generated during the trial is further shown in Fig. 19.

Fig. 18. The concentration of flue gas components during Case 1 trial.

26

Table 11. The flow rate of air and LPG input to the plasma generator and the flue gas composition during Case 1 trial.

Time	Average gas input (Nm³/h)				Average flue gas composition[a]					
	Air plasma	Air forma	LPG forma	Total	CO (ppm)	CO_2 (vol%)	O_2 (vol%)	NO (ppm)	NO_2 (ppm)	H_2O (vol.%)[b]
Sample in										
9.30-10.15	42.8	36.2	2.9	81.9	3	7.7	8.3	7792	1552	8.6
Sample out after 60 & 75 min										
10.30-11.10	38.7	40.0	2.9	81.5	1	7.7	8.4	7619	1639	8.7
Sample out after 120 min										
11.20-14.05	35.0	40.6	2.8	78.5	0	7.7	8.6	7416	1747	8.8
Sample out after 300 min										

[a]in dry flue gas except H_2O
[b]estimated value at 1200 °C, 1 bar
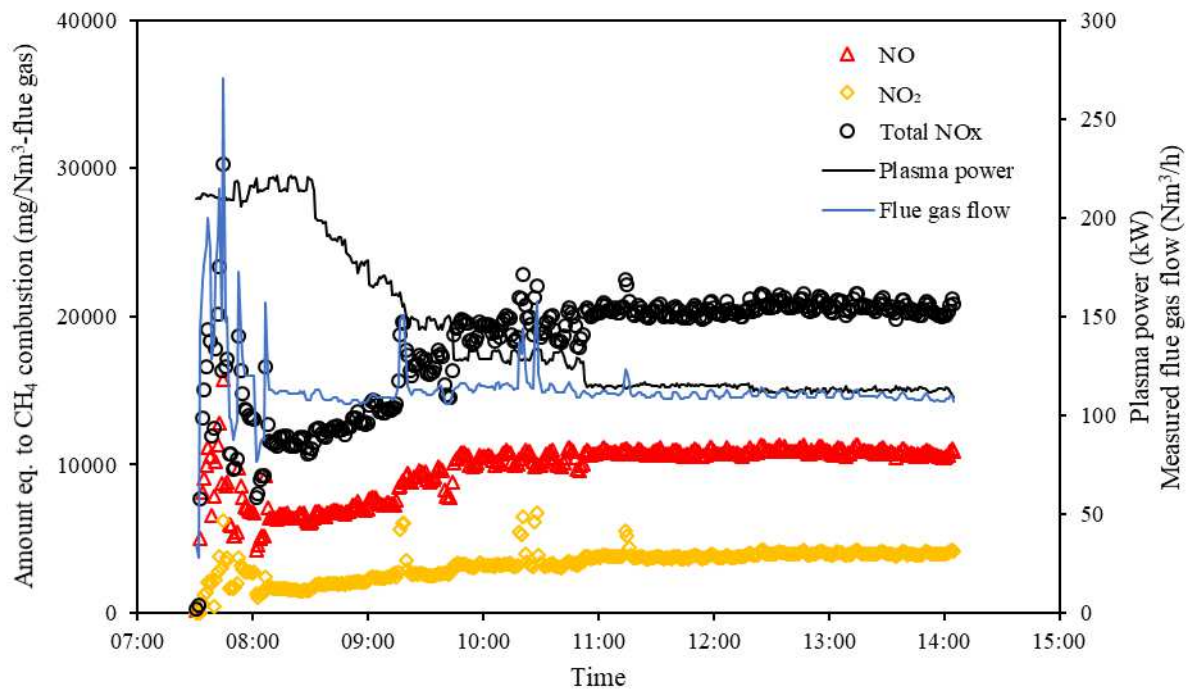
Fig. 19. The amount of the NO_X emission, plasma torch power, and the total calculated flue gas flow during Case 1 trial.

Table 12. The concentration of flue gas's components equivalent to the CH_4 combustion with 3% of excess O_2 (in mg/Nm^3-flue gas and mg/MJ) during steel heating process with air and LPG as plasma gases (Case 1).

Time	Calculated average flowrate eq. to CH_4 combustion (mg/Nm^3-flue gas)						Calculated average flowrate eq. to CH_4 combustion (mg/MJ)					
	CO	CO_2	O_2	NO	NO_2	Total NO_X[a]	CO	CO_2	O_2	NO	NO_2	Total NO_X[a]
Sample in												
9.30-10.15	4	147 267	115 916	10 202	3 116	18 724	1	34 455	27 120	2 387	729	4 381
Sample out after 60 & 75 min												
10.30-11.10	1	157 778	125 694	10 641	3 510	19 791	0	39 379	31 371	2 656	876	4 939
Sample out after 120 min												
11.20-14.05	0	170 338	138 543	11 152	4 028	21 091	0	45 772	37 228	2 997	1 082	5 667
Sample out after 300 min												

[a]NO_2 equivalent

3.4.2 CO_2 as carrier gas

In contrast with the air plasma generator, the use of CO_2 to generate plasma jet can limit the NO_X formation during the heating process. Theoretically, the NO_X formation will not occur as long as there is no air or nitrogen inside the plasma generator or the furnace itself. Nevertheless, during Case 2, it was found that furnace was not correctly sealed, which caused air to enter the furnace. Consequently, the air leak promotes the formation of thermal NO_X. Moreover, the air can also enter the furnace through its windows during the steel samples' unloading process. As shown in Table 13, the gas analyser detected an average amount of NO and NO_2 between 927–1401 and 94–181 ppm, respectively. These values correspond to the total NO_X amount of 1057– 1354 mg/Nm^3-flue gas. The details of the NO_X generated during the trial is further shown in Fig. 21.
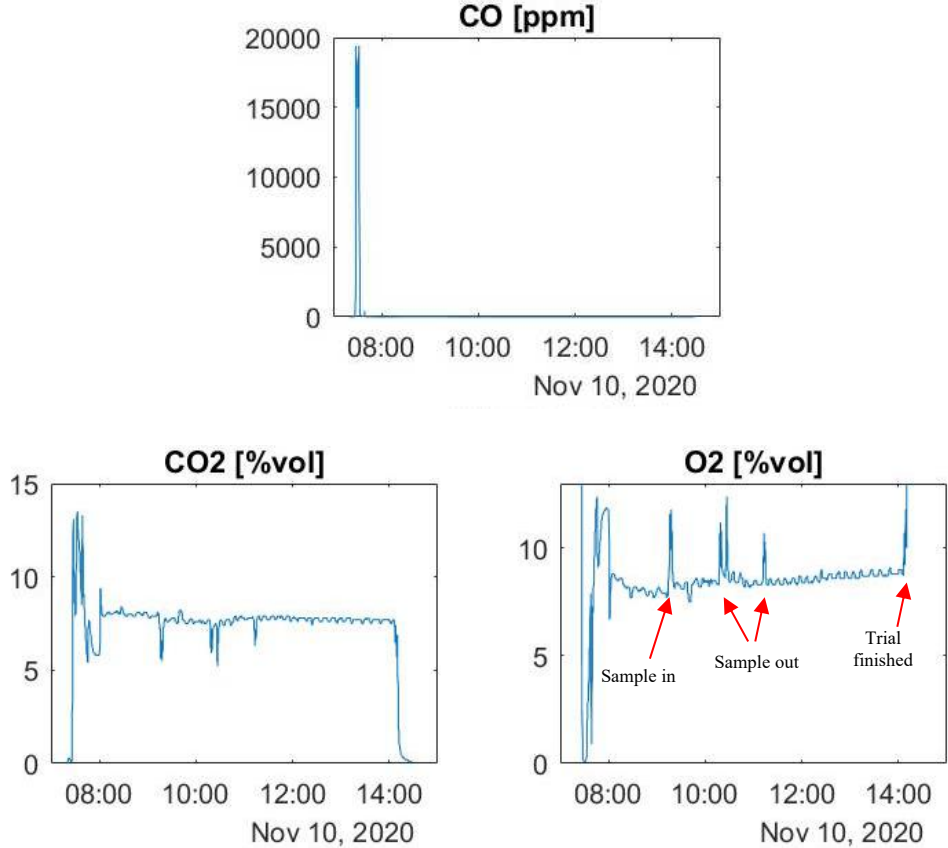

Fig. 20. The concentration of flue gas components during Case 2 trial.

Table 13. The flow rate of CO_2 input to the plasma generator and the flue gas composition during the trial.

| Time	Average gas input (Nm³/h)			Average flue gas composition				
	CO₂ plasma	CO₂ forma	Total	CO (ppm)	CO₂ (%vol.)	O₂ (%vol)	NO (ppm)	NO₂ (ppm)
Sample in								
11.37-12.15	45.5	24.3	69.8	35	82.6	2.6	1401	181
Sample out after 60 & 75 min								
12.45-13.18	36.9	24.2	61.1	41	80.6	3.0	1080	124
Sample out after 120 min								
13.37-16.14	36.3	24.2	60.5	20	82.4	2.7	927	94
Sample out after 300 min								
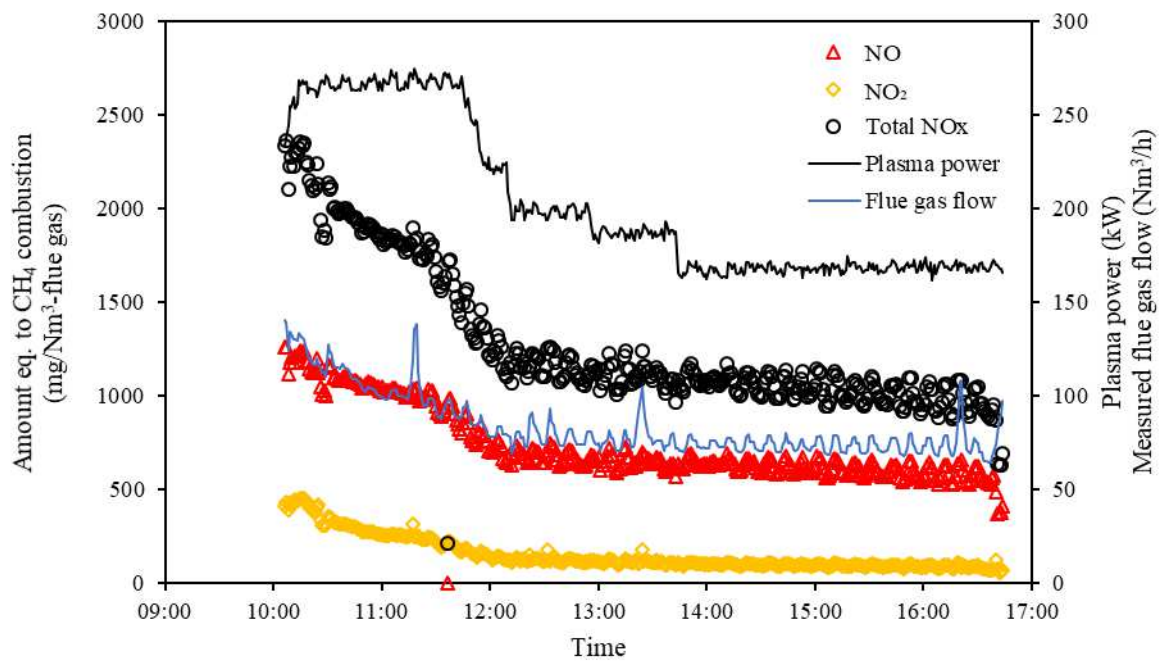
Fig. 21. The amount of the NO$_X$ emission, plasma torch power, and the total calculated flue gas flow during Case 2 trial.

Table 14. The concentration of flue gas's components equivalent to the CH_4 combustion with 3% of excess O_2 (in mg/Nm^3-flue gas and mg/MJ) in during steel heating process with CO_2 as plasma gases (Case 2).

Time	Calculated average flowrate eq. to CH_4 combustion (mg/Nm^3-flue gas)						Calculated average flowrate eq. to CH_4 combustion (mg/MJ)					
	CO	CO_2	O_2	NO	NO_2	Total NO_X[a]	CO	CO_2	O_2	NO	NO_2	Total NO_X[a]
Sample in												
11.37-12.15	18	677 471	15 555	784	155	1 354	1.8	67 722	1 555	78	15	135
Sample out after 60 & 75 min												
12.45-13.18	24	731 542	19 709	668	117	1 140	2.6	80 876	2 179	74	13	126
Sample out after 120 min												
13.37-16.14	13	817 792	19 438	627	98	1 057	1.5	98 892	2 351	76	12	128
Sample out after 300 min												

[a]NO_2 equivalent

3.4.3 N₂ as carrier gas

Based on the Case 2 trial experience, some improvements were made to prevent air leaks from coming into the furnace. These improvements include adding more seals to the furnace's wall gap/borders. Moreover, a brick wall was added at the furnace's outlet to increase the pressure of the furnace; hence; air from the outside could not enter the furnace.

Nevertheless, a significant amount of NO_X can still be found in the flue gas despite the sealing improvements. As shown in Table 15, the highest average amount of NO could reach 2989 ppm, which obtained during 12.36–14.57 when 57.4 Nm^3/h of N_2 was being supplied as plasma gas. The data in the table also suggests that the NO_X concentration can be reduced by increasing the N_2 flow. For instance, during 15.07–15.11, the N_2 flow increased by 16% to 66.8 $Nm3$/h and caused the NO content to decrease by 34% to 1973 ppm. A further reduction to only 588 ppm could be achieved during 15.16–15.23 when the total N_2 flow was raised to 86.3 Nm^3/h. This NO_X reduction was possible due to the increase in the furnace pressure following the rise of the N_2 flow; hence, the furnace became more airtight.

In general, the total NO_X concentration ranged between 717–2511 mg/Nm^3-flue gas during the trial, as presented in Table 16. At approximately 70 Nm^3/h of N_2 flow, the total NO_X concentration was 1622 mg/Nm^3-flue gas. This value was higher than that of CO_2 plasma generation (Case 2) with a total NO_X concentration of 1354 mg/Nm^3-flue gas at a similar plasma gas flow. The details of the NO_X generated during the trial is further shown in Fig. 23.
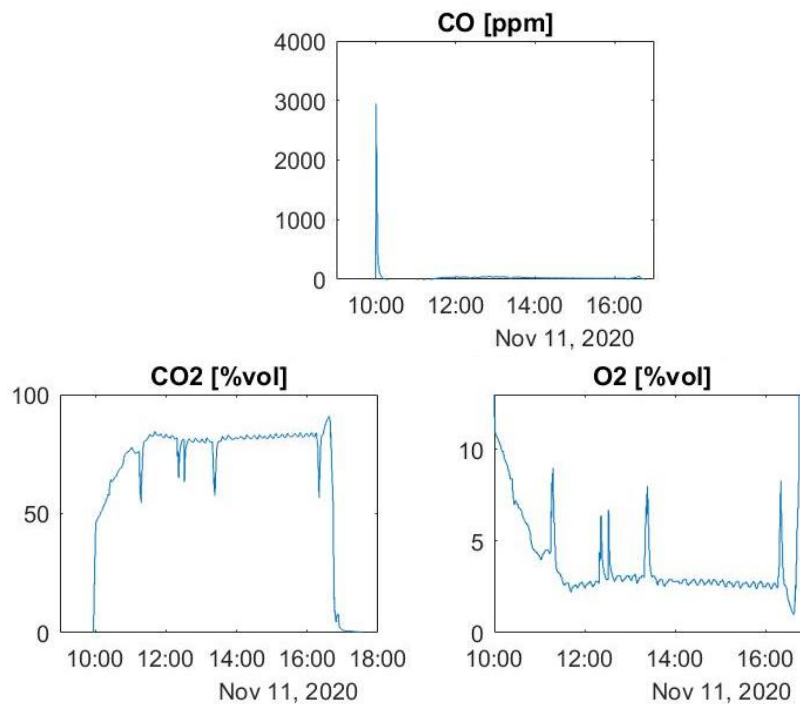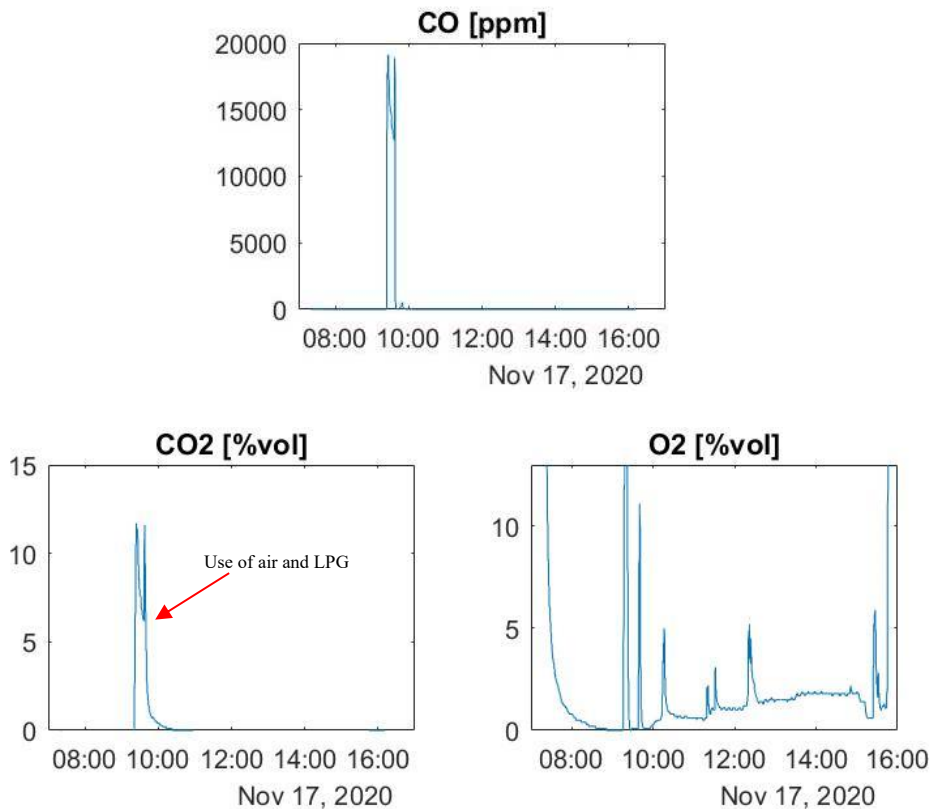

Fig. 22. The concentration of flue gas components during Case 3 trial.

Table 15. The flow rate of N_2 input to the plasma generator and the flue gas composition during the trial.

Time	Average gas input (Nm³/h)			Average gas composition				
	N_2 plasma	N_2 forma	Total	CO (ppm)	CO_2 (%vol.)	O_2 (%vol)	NO (ppm)	NO_2 (ppm)
Sample in								
10.34-11.15	80.0	0	80.0	0	0	0.6	1186	21
Sample out after 60 & 75 min								
11.42-12.08	70.3	0	70.3	0	0	1.1	2011	73
Sample out after 120 min								
12.36-14.57	57.4	0	57.4	0	0	1.7	2989	200
Plasma gas flow is increased								
15.07-15.11	66.8	0	66.8	0	0	1.4	1973	91
Forma and plasma gas flow are increased								
15.16-15.23	65.2	21.1	86.3	0	0	0.6	588	17
Sample out after 300 min								
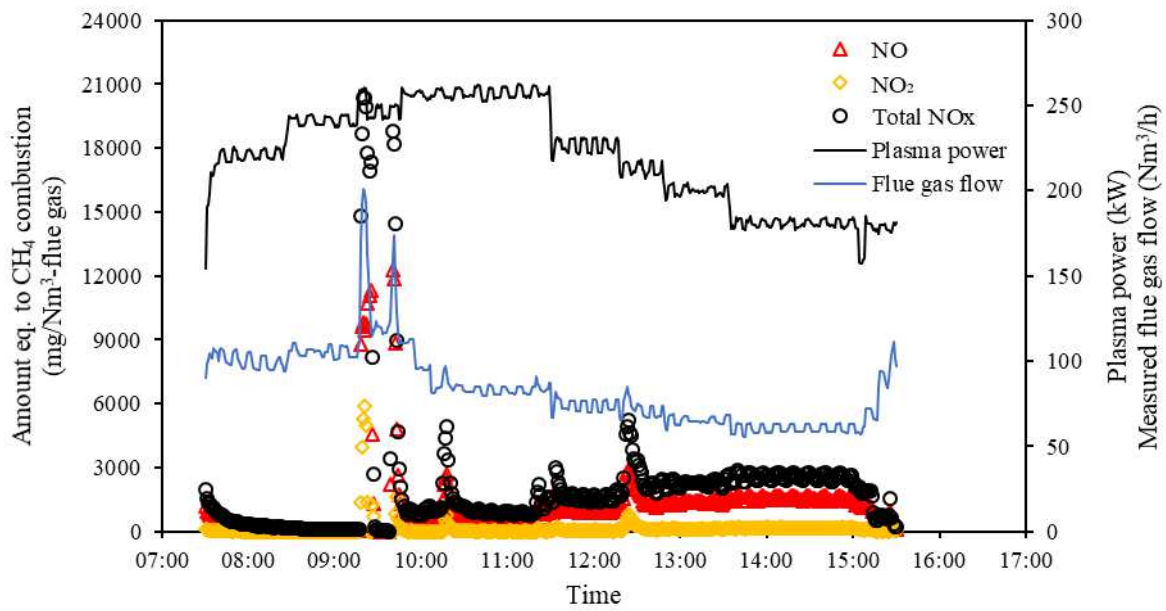
Fig. 23. The amount of the NO_X emission, plasma torch power, and the total calculated flue gas flow during Case 3 trial.

Table 16. The concentration of flue gas's components equivalent to the CH_4 combustion with 3% of excess O_2 (in mg/Nm³-flue gas and mg/MJ) during steel heating process with N_2 as plasma and forma gases (Case 3).

Time	Calculated average flowrate eq. to CH_4 combustion (mg/Nm³-flue gas)						Calculated average flowrate eq. to CH_4 combustion (mg/MJ)					
	CO	CO₂	O₂	NO	NO₂	Total NOₓ[a]	CO	CO₂	O₂	NO	NO₂	Total NOₓ[a]
Sample in												
10.34-11.15	0	0	3 340	593	16	924	0	0	299	53	1	88
Sample out after 60 & 75 min												
11.42-12.08	0	0	5 713	1 023	57	1 622	0	0	519	93	5	147
Sample out after 120 min												
12.36-14.57	0	0	9 204	1 538	158	2 511	0	0	847	142	14	231
Plasma gas flow is increased												
15.07-15.11	0	0	9 190	1 215	85	1 944	0	0	1 011	134	9	214
Forma and plasma gas flow are increased												
15.16-15.23	0	0	4 958	456	20	717	0	0	686	63	3	99
Sample out after 300 min												

[a]NO₂ equivalent

3.4.4 CO_2 and H_2O as carrier gases

Table 17 presents the flue gas composition obtained from Case 4 experiment. In this case, the use of CO_2 and H_2O could limit the generation of NO_X gases as their concentration was lower than in any other cases. The NO and NO_2 amount were between 510 – 635 and 46 – 53 ppm, respectively. These values correspond to no more than 490 mg/Nm^3-flue gas of total NO_X (see Table 18). Unfortunately, Case 4 could not be fairly compared to Case 2 due to the difference in the degree of air leakage. Hence, no clear conclusion can be made on the effect of adding steam to the CO_2 plasma generation in term of the generated emission. The details of the NO_X generated during the trial is further shown in Fig. 25.
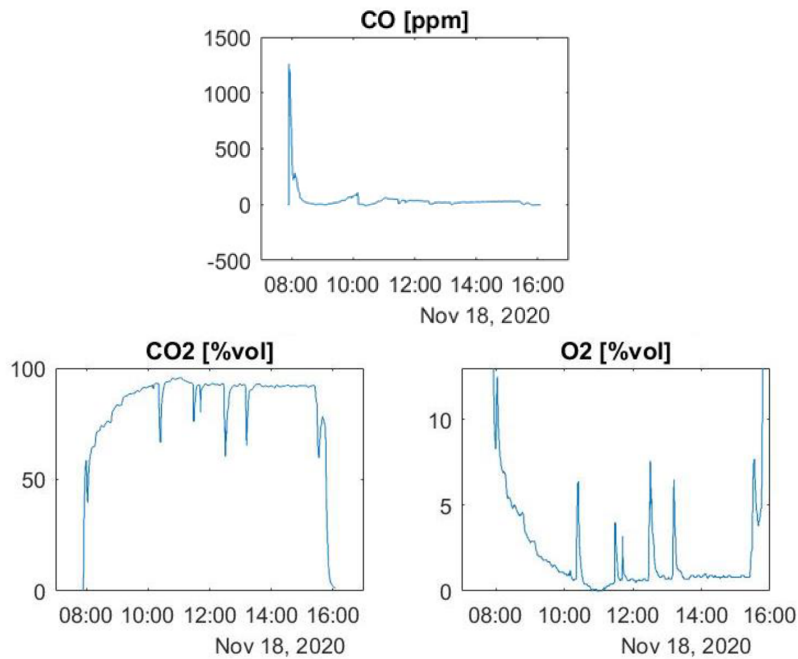
Fig. 24. The concentration of flue gas components during Case 4 trial.

Table 17. The flow rate of CO_2 and H_2O input to the plasma generator and the flue gas composition during the trial.

Time	Average gas input (Nm^3/h)				Average flue gas composition[a]					
	CO_2 plasma	CO_2 forma	Total CO_2	H_2O (kg/h)	CO (ppm)	CO_2 (%vol.)	O_2 (%vol)	NO (ppm)	NO_2 (ppm)	H_2O (vol.%)[b]
Sample in										
10.40-11.20	51.1	16.1	67.2	36	40	94.8	0.1	635	53	54.4
Sample out after 60 & 75 min										
11.50-12.25	44.3	16.2	60.5	36	34	92.7	0.6	565	50	56.5
Sample out after 120 min										
12.50-13.08	44.4	16.2	60.6	36	19	92.4	0.8	553	49	56.2
Sample out after 170 min										
13.37-15.23	40.6	16.2	56.8	36	26	92.0	0.8	510	46	57.7
Sample out after 300 min										

[a]in dry flue gas except H_2O

Fig. 25. The amount of the NO_X emission, plasma torch power, H_2O input flow, and the total calculated flue gas flow during Case 4 trial.

Table 18. The concentration of flue gas's components equivalent to the CH_4 combustion with 3% of excess O_2 (in mg/Nm^3-flue gas and mg/MJ) during steel heating process with CO_2 as plasma gas and H_2O as forma gas (Case 4).

Time	Calculated average flowrate eq. to CH₄ combustion (mg/Nm³-flue gas)						Calculated average flowrate eq. to CH₄ combustion (mg/MJ)					
	CO	CO₂	O₂	NO	NO₂	Total NOₓ[a]	CO	CO₂	O₂	NO	NO₂	Total NOₓ[a]
Sample in												
10.40-11.20	17	626 829	654	286	37	475	1.4	50 504	53	23	3	38
Sample out after 60 & 75 min												
11.50-12.25	16	704 649	3 468	293	39	488	1.5	65 276	321	27	4	45
Sample out after 120 min												
12.50-13.08	9	705 166	4 238	288	39	480	0.9	65 581	394	27	4	45
Sample out after 170 min												
13.37-15.23	13	710 320	4 704	269	37	448	1.2	66 858	443	25	3	42
Sample out after 300 min												

[a]NO_2 equivalent

3.4.5 N_2 and H_2O as carrier gases

Table 19 and Table 20 shows the flue gas composition obtained from Case 5 in which H_2O was added to the N_2 plasma generation. It should be noted that the flow rate of N_2 in this case (>100 Nm^3/h) was higher than that of Case 3. As a result, it can be seen that the NO$_X$ concentration was significantly higher than that of Case 3. Specifically, the total NO$_X$ value was around 5500 mg/Nm^3-flue gas, which is at least double that of Case 3. The details of the NO$_X$ generated during the trial is further shown in Fig. 27.
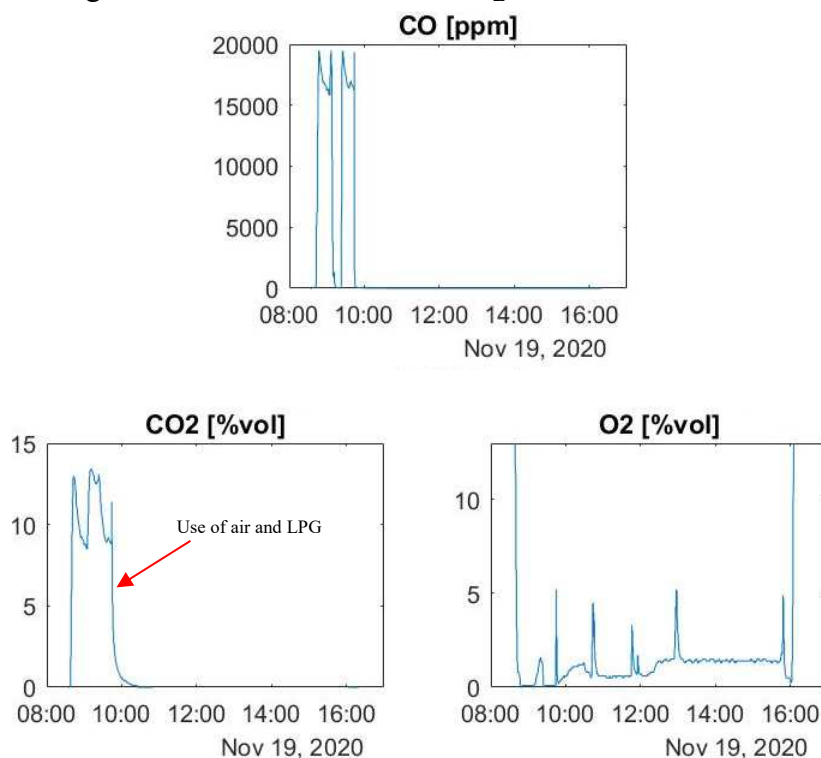
Fig. 26. The concentration of flue gas components during Case 5 trial.

Table 19. The flow rate of N_2 and H_2O input to the plasma generator and the flue gas composition during the trial.

Time	Average gas input (Nm^3/h)				Average flue gas composition[a]					
	N_2 plasma	N_2 forma	Total N_2	H_2O (g/h)	CO (ppm)	CO_2 (%vol.)	O_2 (%vol)	NO (ppm)	NO_2 (ppm)	H_2O (vol.%)[b]
Sample in										
10.52-11.44	85.0	30.2	115.2	36	0	0	0.6	4890	272	31.9
Sample out after 60 & 75 min										
12.01-12.21	82.9	29.5	112.5	36	0	0	0.7	4699	422	32.3
12.21-12.52	75.2	30.2	105.4	36	0	0	1.4	3973	707	33.0
Sample out after 135 min										
13.10-15.40	75.1	30.0	105.0	36	0	0	1.4	4037	820	33.1
Sample out after 300 min; H_2O flow is doubled										
15.53-15.59	73.9	30.7	104.5	72	0	0	0.5	8112	0	50.7

[a]in dry flue gas except H_2O
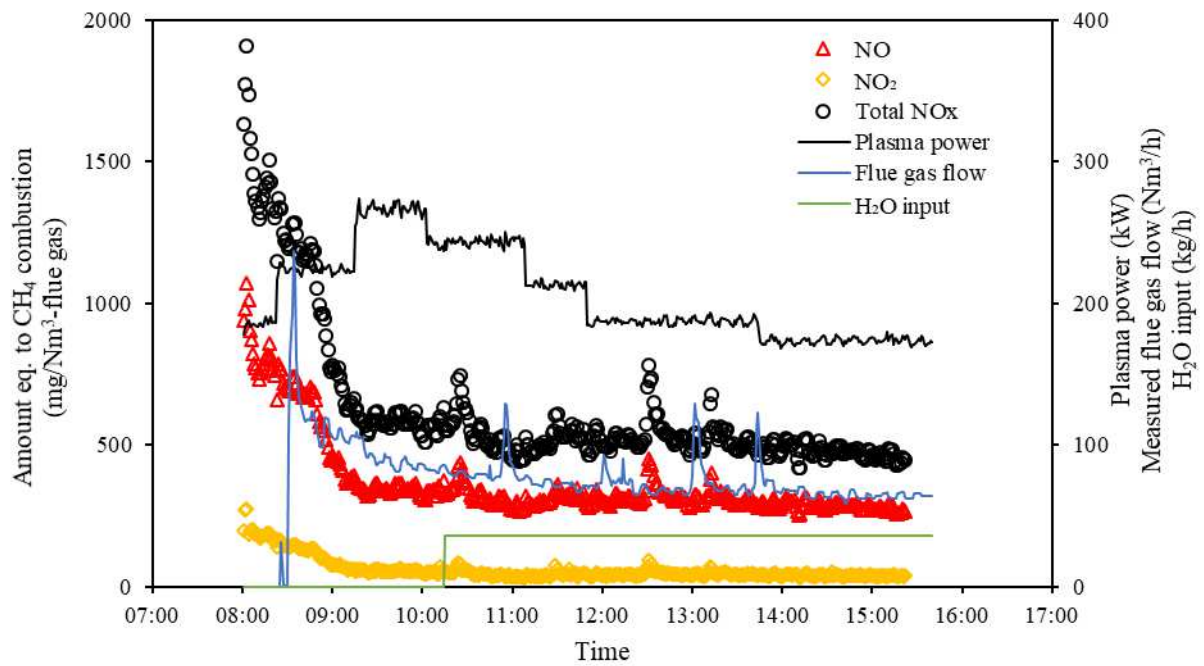[b]estimated value at 1200 °C, 1 bar

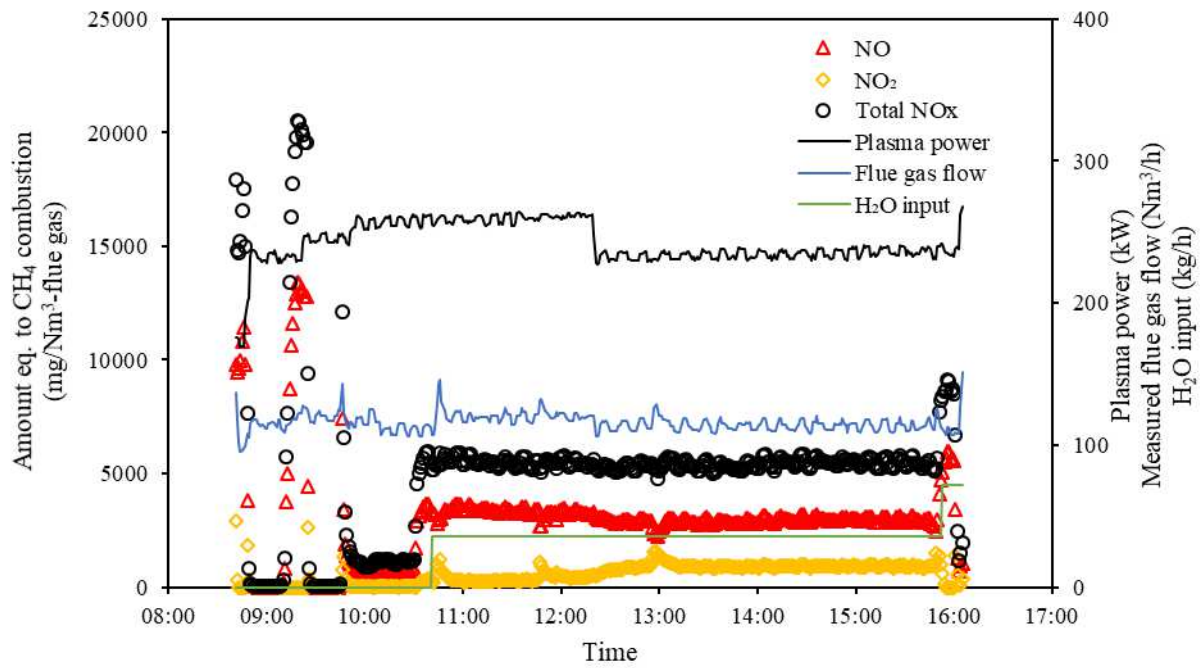Fig. 27. The amount of the NO$_X$ emission, plasma torch power, H$_2$O input flow, and the total calculated flue gas flow during Case 5 trial.

Table 20. The concentration of flue gas's components equivalent to the CH_4 combustion with 3% of excess O_2 (in mg/Nm³-flue gas and mg/MJ) during steel heating process with N_2 as plasma gas and H_2O as forma gas (Case 5).

Time	Calculated average flowrate eq. to CH_4 combustion (mg/Nm³-flue gas)						Calculated average flowrate eq. to CH_4 combustion (mg/MJ)					
	CO	CO₂	O₂	NO	NO₂	Total NOₓ[a]	CO	CO₂	O₂	NO	NO₂	Total NOₓ[a]
Sample in												
10.52-11.44	0	0	4 411	3 511	299	5 670	0	0	566	450	38	727
Sample out after 60 & 75 min												
12.01-12.21	0	0	5 221	3 353	462	5 592	0	0	666	428	59	713
12.21-12.52	0	0	11 079	3 012	822	5 430	0	0	1 501	408	111	736
Sample out after 135 min												
13.10-15.40	0	0	11 270	3 030	944	5 580	0	0	1 512	406	127	748
Sample out after 300 min; H_2O flow is doubled												
15.53-15.59	0	0	3 915	5 854	0	8 957	0	0	505	755	0	1155

[a]NO_2 equivalent

3.4.6 Summary of the emission results
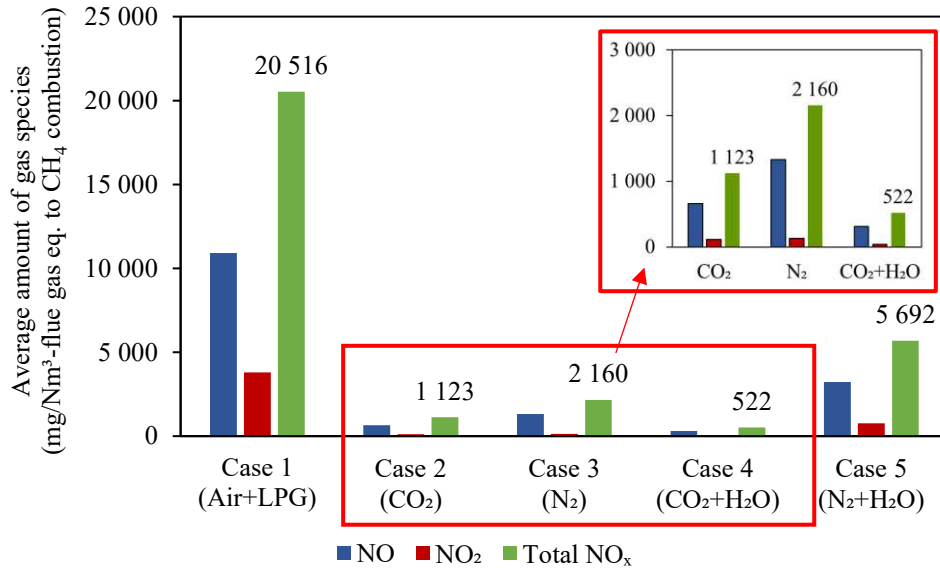
Fig. 28. Comparison of NO_X emission produced from different cases during 300 min of steel heat-treatment presented in mg/Nm³-flue gas eq. to CH_4 combustion.
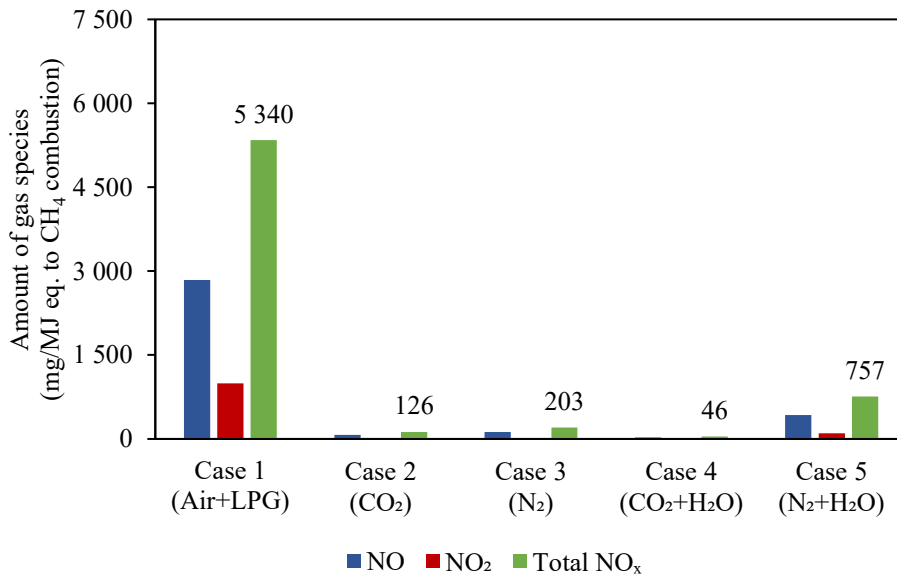
Fig. 29. Comparison of NO_X emission produced from different cases during 300 min of steel heat-treatment presented in mg/MJ eq. to CH_4 combustion.

Based on the results of the conducted tests, the following conclusions on the furnace emission can be made.

- The use of air for plasma carrier gas generates the highest NO_X amount in the flue gas due to the extensive thermal NO_X formation in a N_2-O_2 rich atmosphere.
- Combination of CO_2 and H_2O potentially produces the lowest NO_X emission (522 mg/Nm³ or 46 mg/MJ eq. to CH_4 combustion) than other investigated gas mixtures (see Fig. 28 and

Fig. 29). Nevertheless, it should be noted that during the trial with pure CO_2 carrier gas, there was higher amount of air leakage, which caused the process to generate higher amount of NO_X than that of the CO_2-H_2O case.

- The lowest NO_X emission value obtained from the pilot trial (522 mg/Nm^3) is still higher than the typical ranges of the NO_X emissions according to the best available technology references (see Table 21). It should be noted that the plasma torch used in the pilot trials was not specifically optimized for such operations; hence, the NO_X emission was relatively high.
- In this pilot plant study, the primary source of the NO_X emission when using the CO_2, H_2O, or N_2 plasma torch is the air leakage. This can be prevented further by optimising the operating conditions of the furnace, such as adjusting the pressure of the furnace chamber.

Table 21. The range of the NO_X emissions according to the EU's best available technology reference documents (BREF).

Processes	Range of NOX emission (mg/Nm^3)	References
Coke oven plants	350-500 (<10 years old plants), 500-650 (older plants)	EU BREF[4]
Blast furnaces	<100	EU BREF[4]
Combustion boiler (biomass)	40-225 (yearly average)	EU BREF[5]
Combustion boiler (coal/oil)	45-270 (yearly average)	EU BREF[5]
Combustion boiler/engine (natural gas)	10-100 (yearly average)	EU BREF[5]
Combustion boiler (iron & steel process gases)	15-100 (yearly average)	EU BREF[5]

3.4.7 Possible NO$_X$ reduction methods

As pointed out in the pilot trial results, the application of the thermal plasma torch in a steel heat-treatment furnace should be carefully designed to limit the NO_X emission. The process should be optimized by considering the well-established methods of NO_X reduction. In general, the methods for the reduction of NO_X emission can be divided into primary and secondary methods.

The primary methods mainly involve the optimization or adjustment of the combustion processes to eliminate the NO_X at its source. In the case of plasma heating, these reduction methods can be focused on limiting the formation of fuel-NO_X and thermal-NO_X due to the presence of nitrogen in a very high plasma jet temperature. As listed in Table 22, fuel-NO_X can be avoided by limiting the presence of nitrogen in the plasma gas carrier. Meanwhile, the formation of thermal-NO_X can be reduced by diluting the high-temperature zone around the

---

[4] European Commission. Establishing the best available techniques (BAT) conclusions under Directive 2010/75/EU of the European Parliament and of the Council on industrial emissions for iron and steel production. 2012.

[5] European Commission. Establishing best available techniques (BAT) conclusions, under Directive 2010/75/EU of the European Parliament and of the Council, for large combustion plants. 2017.

plasma jet with use of very intensive internal flue gas recirculation as illustrated in Fig. 30. In this case, the jet temperature can be reduced which leads to the reduction of NO_X formation. It could also result in a bigger flame volume; hence, more uniform heating zone can be achieved. This method has been well-established, especially in the field of high-temperature oxy-fuel combustion technology, and can effectively reduce the NO_X emission. In addition, the primary methods are the more cost effective way than the secondary one. Even though there will be a additional CAPEX for optimizing the plasma torch, using primary methods typically will not increase OPEX, as no additional operational substances are required.

Table 22. Primary methods for NO_X reduction in the case of thermal plasma torch.

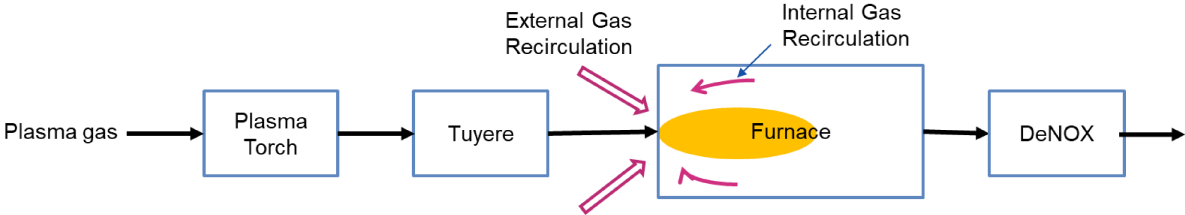| NO_X formation mechanism	Possible mitigations
Fuel NO_X	Limiting the N_2 in the plasma gas carriers.
Thermal NO_X	Reducing the torch temperature by intensive internal/external gas recirculations.
Prompt NO_X	Not relevant in the case of plasma heating.

Fig. 30. Illustration of the possible methods for NO_X reduction during a plasma heating process.

In the secondary method, a removal process is added to reduce the NOx compounds that are already formed in the combustion process. Commonly known as DeNOX process, this method can be divided into two types: the Selective Catalytic Reduction (SCR) and Selective Non-catalytic Reduction (SNCR). The SCR process can typically reduce the NOx emission up to more than 90% efficiency, while the SNCR can only reduce the NOx emission to up to 60%.

4   CONCLUSION AND RECOMMENDATION

4.1 Conclusion

A series of pilot-scale experiment has been successfully performed to investigate the application of plasma torches for steel-heat treatment. Different plasma carrier gases' performance has been examined in terms of its impact on the furnace heating rate, steel sample heating rate, and the flue gas emission. Based on the results of this study, the following conclusion can be made.

- The plasma torch efficiency trend is related to the specific heat capacity of the plasma gas carrier, in which a higher specific heat capacity causes a higher efficiency. This is especially true in the case of our pilot-scale tests as the plasma torch was not specifically designed for the tested carrier gases. Without the presence of additional energy from LPG, CO_2 as a plasma gas carrier resulted in the highest plasma torch efficiency than other gas carrier tested in this study.

- Combination of air and LPG in the plasma generator provides the best heating performance in terms of the uniform temperature distribution and higher heating rate, followed by CO_2-based plasma generator. At the end those trials, the temperature of the furnace varied approximately 20 °C, which is within an acceptable range. Furthermore, a combination of N_2 and H_2O is least favourable due to the poorer temperature distribution and lower heating rate.

- The core temperature of the steel sample could reach ~1200 °C in all cases. It suggests that the steel sample could be uniformly heated to the same temperature of the furnace chamber.

- Despite the superior heating rate, air and LPG use in the plasma torch generates the highest NO_X amount in the flue gas due to the extensive thermal NO_X formation in a N_2-O_2 rich atmosphere. Combination of CO_2 and H_2O potentially produces the lowest NO_X emission (522 mg/Nm^3 eq. to CH_4 combustion) than other investigated gas mixtures.

- It can be concluded that CO_2, regardless the H_2O addition, is the most promising plasma carrier gas as it can provide a good heat transfer with a possibility to prevent the NO_X emission.

4.2 Recommendation for future research/application

Continuous research focusing on the development of highly efficient and NO_X-free plasma heated furnace are recommended. The following aspects can be considered.

- A fundamental study such as Computational Fluid Dynamics (CFD) simulation could be useful to understand further the heat transfer phenomenon inside the furnace chamber at different operating parameters of the plasma torch.

- A further lab- or pilot-scale trial should be done systematically to understand and confirm the hypotheses that are suggested by this technical report. The control variable should be properly fixed in order to test the relative relationship of the dependent (e.g., heat flux, furnace temperature, etc.) and independent variables (e.g., plasma power, carrier gas flow, etc.).

- More attention should be given to prevent the exposure of the furnace chamber to the outside air in order to eliminate the NO_X formation. This can be done by optimizing the operating parameter of the furnace such as adjusting the pressure, etc.

- Process optimization can be done to improve the thermal efficiency of the plasma-based furnace. The plasma torch should also be optimized based on the selected carrier gas to ensure an optimum efficiency.